Study of the effectiveness of a ZnO–TiO₂ formulation in the degradation of humic substances in mature leachate by solar photocatalysis Brazil

Nicoly Milhardo Lourenço Nohara[1] ; **Helcio José Izário Filho[1]** ;
Adriano Francisco Siqueira[2] ; **Leandro Gonçalves de Aguiar[1]** ;
Gabriel Caracciolo Koenigkam de Oliveira[1] ; **Evandro Luís Nohara[3]** ;
Marco Aurélio Kondracki de Alcântara[2]* ;
Diovana Aparecida dos Santos Napoleão[2]

[1]Departamento de Engenharia Química. Escola de Engenharia de Lorena (EEL-USP), Estrada Municipal do Campinho, n° 100, CEP: 12602-810, Lorena, SP, Brazil. E-mail: nicoly.nohara@gmail.com, helcio_izario@usp.br, leandroaguiar@usp.br, gabrielcaracciolo@hotmail.com
[2]Departamento de Ciências Básicas e Ambientais. Escola de Engenharia de Lorena (EEL-USP), Estrada Municipal do Campinho, n° 100, CEP: 12602-810, Lorena, SP, Brazil.
E-mail: adrianoeel@usp.br, diovana@usp.br
[3]Departamento de Engenharia Mecânica. Universidade de Taubaté (UNITAU), Rua Daniel Danelli, s/n, (Campus da Juta), CEP: 12060-440, Taubaté, SP, Brazil. E-mail: evandro.nohara@unitau.com.br
*Corresponding author. E-mail: marko@usp.br

ABSTRACT

Treatment of landfill leachate is an important environmental issue, especially in developing countries such as Brazil. Advanced oxidation processes (AOPs) have been considered interesting treatment alternatives. In this study, ZnO–TiO₂ mixtures were incorporated into a paint polymer matrix and fixed onto supports. Paints were applied by overlapping coat layers on plates, resulting in high film thickness (600 ± 80 µm). Treatment of mature leachate by an AOP was conducted in a plug flow reactor connected to a stirred tank under solar irradiation. The objective was to evaluate the degradation of humic acid (HA) and fulvic acid + humins (FAH). The highest HA and FAH removal efficiencies were $62\% \pm 4.9\%$ and $16\% \pm 4.2\%$, respectively. The kinetic model provided a coefficient of determination (R^2) of 0.974. Rate constants for HA and FAH removal were 2.96 and 1.03×10^{-3} min^{-1}, respectively. Statistical models for HA and FAH degradation had R^2 values of 0.96 and 0.99, respectively. Both approaches indicated that HA degradation is greater at acidic pH and higher TiO₂ concentrations. FAH degradation was favored by acidic pH and higher ZnO concentrations. Statistical models showed the same mean difference in conversion between replicate runs of HA and FAH, suggesting a uniform diffusion of fractions through catalysts.

Keywords: heterogeneous photocatalysis, humic and fulvic acid, landfill leachate treatment, titanium dioxide, zinc oxide.

Estudo da eficácia de uma formulação ZnO–TiO2 na degradação de substâncias húmicas em chorume maduro por fotocatálise solar

RESUMO

O tratamento de chorume de aterro é uma questão ambiental importante, especialmente em países em desenvolvimento como o Brasil. Os processos oxidativos avançados (POA) têm sido considerados interessantes alternativas de tratamento. Neste estudo, misturas de ZnO–TiO2 foram incorporadas a uma matriz polimérica de tinta e fixadas em suportes. As tintas foram aplicadas pela sobreposição de camadas de revestimento em placas, resultando em alta espessura de filme ($600 \pm 80 \, \mu m$). O tratamento do lixiviado maduro por um POA foi conduzido em um reator de fluxo contínuo conectado a um tanque de agitação sob irradiação solar. O objetivo foi avaliar a degradação de ácido húmico (HA) e ácido fúlvico + huminas (FAH). As maiores eficiências de remoção de HA e FAH foram 62% $\pm$ 4,9% e 16% $\pm$ 4,2%, respectivamente. O modelo cinético forneceu um R^2 de 0,974. As constantes de velocidade para remoção de HA e FAH foram 2,96 e 1,03 $\times$ 10^{-3} min^{-1}, respectivamente. Os modelos estatísticos para degradação de HA e FAH tiveram valores de R^2 de 0,96 e 0,99, respectivamente. Ambas as abordagens indicaram que a degradação do HA é maior em pH ácido e concentrações mais altas de TiO2. A degradação de FAH foi favorecida por pH ácido e maiores concentrações de ZnO. Os modelos estatísticos mostraram a mesma diferença significativa na conversão entre as execuções repetidas, sugerindo uma difusão uniforme das frações através dos catalisadores.

Palavras-chave: ácido húmico e fúlvico, dióxido de titânio, fotocatálise heterogênea, óxido de zinco, tratamento de lixiviados de aterros sanitários.

1. INTRODUCTION

Municipal solid waste is commonly sent to landfills or incinerators. Incineration processes are mostly used in European countries. An advantage of incinerators is that they occupy small areas compared with landfills, but a disadvantage is the generation of persistent organic pollutants (Tait *et al.*, 2020). In many countries, including Brazil, solid waste is disposed of in open dumping sites, and only a small amount is discarded in sanitary landfills (Costa *et al.,* 2019; Ye *et al.,* 2018). Widely used in Brazil, landfills allow the reuse of methane gas but require large areas and generate leachate, a liquid composed predominantly of natural organic matter, which, without adequate treatment and disposal, causes numerous negative impacts on the environment (Costa *et al.*, 2019).

Leachate composition varies according to environmental conditions, waste source, and landfill age. Leachate from landfills with more than 10 years of operation is classified as mature. The maturation period represents a critical phase for leachate physicochemical properties (Peng, 2017: Luo *et al.*, 2020), characterized by an increase in humic substances (humic acids, fulvic acids, and humins) and ammonia nitrogen, alkalization (pH > 8.0), and initiation of methane production (methanogenic phase) (Costa *et al.*, 2019). At this stage, it is not possible to mineralize the entire organic load through biological treatment, given the recalcitrance of humic substances (Costa *et al.*, 2019), which are predominantly composed of aromatic and aliphatic compounds containing carbon, oxygen, nitrogen, and sulfur (e.g., phenols and carboxylic acids) (Nguyen *et al.*, 2020).

Different methods are available for treating and discarding waste. A detailed analysis of the results of leachate treatment by different processes can be found in recent review studies (Wang *et al.*, 2013; Song *et al.*, 2023). Advanced oxidation processes (AOPs), particularly heterogeneous photocatalysis, show promise as complementary treatments to biological

Rev. Ambient. Água vol. 18, e2932 - Taubaté 2023

IPABH

processes in sanitary landfills (Turkten and Bekbölet, 2020; Silva *et al.*, 2022). Hassan *et al.* (2016), in a review article, highlighted that heterogeneous photocatalysis with the semiconductor TiO_2 afforded satisfactory degradation of several recalcitrant compounds from landfill leachates. Good results were also obtained with ZnO in a study by Mohd Omar *et al.* (2014). One way to achieve even more promising results is to combine these semiconductors. $ZnO-TiO_2$ mixtures have high ability to absorb UV radiation (including visible spectrum wavelengths) and reduce the recombination of electron–hole pairs, which, in turn, increases charge separation and photocatalytic activity (Di Mauro *et al.*, 2017); Byrne *et al.*, 2018; Turkten and Bekbölet, 2020). These mixtures can be used in suspension or fixed on a stationary support, the latter being the most economical option because it eliminates the need for filtration steps. $ZnO-TiO_2$ mixtures can be fixed on supports by incorporation into a polymer matrix, such as acrylic paints, allowing application in open reactors operated under solar irradiation.

Removal of organic matter by photocatalysis with TiO_2 or ZnO has been carried out for more than two decades. Some studies combined semiconductors for the photodegradation of synthesized humic acids (Wang *et al.*, 2013; Zulfikar *et al.*, 2020; Turkten and Bekbölet, 2020) or dissolved organic matter (Li *et al.*, 2022) under solar irradiation or artificial light. Bah *et al.* (2023) found that there are few studies on photocatalysis with sunlight as the irradiation source. So far, there is no report of the combination of TiO_2 and ZnO via heterostructures or binary mixtures for the photodegradation of humic substances in mature landfill leachate using sunlight as the light source.

The oxidation kinetics of humic acids (HA), fulvic acids (FA), and humins have been studied using different techniques, including photoelectrocatalytic processes (Selcuk *et al.*, 2003), TiO_2/activated carbon photocatalysis (Xue *et al.*, 2011), and ZnO nano photocatalysis (Oskoei *et al.*, 2016). The use of sunlight for photocatalysis of humic substances has also been explored (He, 2013). In a recent study, a $ZnO-TiO_2$ nanocomposite was applied for the photocatalysis of humic substances, and different reaction orders were tested (Turkten and Bekbölet, 2020). The pseudo-first order kinetic constant of the binary mixture was found to be $0.902–0.735.10^{-2}$ min^{-1} for HA degradation, as assessed by determining non-purgeable organic carbon levels. The simplified photocatalysis mechanism of these mixtures was illustrated by the authors, as follows Equations (1, 2, 3, 4, 5 and 6):

$$ZnO\text{-}TiO_2 + hv \longrightarrow h_{VB^+} + e_{CB^-} \tag{1}$$

$$h_{VB^+} + H_2O \longrightarrow OH^. + H^+ \tag{2}$$

$$e_{CB^-} + O_2 \longrightarrow O_2^{.-} \tag{3}$$

$$O_2^{.-} + H^+ \longrightarrow HO_2^. \tag{4}$$

$$2HO_2^. \longrightarrow H_2O_2 + O_2 \tag{5}$$

$$H_2O_2 + e_{CB^-} \longrightarrow OH^. + OH^- \tag{6}$$
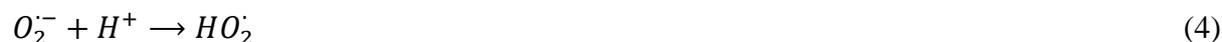
Some studies, such as that of Brito *et al.* (2019), investigated the kinetics of photocatalytic degradation of organic load in leachates; however, there is a knowledge gap regarding the specific degradation kinetics of HA, FA, and humins by heterogeneous photocatalysis with $ZnO-TiO_2$. This study therefore aimed to investigate the decomposition of HA and FA + humins (FAH) in landfill leachate by heterogeneous photocatalysis using binary mixtures of $ZnO-TiO_2$ at different pH ranges under sunlight. Kinetic and statistical approaches were used. The catalyst was obtained by a simple, low-input method, adding value to the final result. The results of this study can be used as a basis for future research on the photocatalysis of HA, FA, and humins from mature landfill leachate.

IPABH

2. MATERIALS AND METHODS

Binary mixtures of the photocatalyst were prepared by simple mixing. The inputs used for preparation of photocatalytic materials were acrylic paint (60% w/v), photocatalysts (ZnO–TiO$_2$, 20% w/v), deionized water (15% w/v), ammonium polyacrylate (PAA–NH$_4$, 4% w/v), and carboxymethylcellulose (CMC, 1% w/v). The commercial acrylic paint was colorless, semi-gloss, and water-soluble. The paint is mainly composed of methyl methacrylate copolymer, butyl acrylate, 2-hydroxyethyl methacrylate, and acrylic acid at a weight ratio of 60:22.2:10:7.8, with an average molar weight of 15,000 to 35,000 g mol^{-1} (Jones *et al.*, 2017). Regarding photocatalysts, which also served as pigments, TiO$_2$ had a purity of 99.9% (J.T. Baker) and was composed of mixed phases (60% anatase and 40% rutile). ZnO had a purity of 99.5% (synthesized at the Department of Chemical Engineering, Lorena School of Engineering, University of São Paulo, Brazil), and the predominant phase was wurtzite (>90%). The weight composition of the solid binary mixtures used in this study was as follows: (a) 1–65% ZnO + 35% TiO$_2$, (b) 2–20% ZnO + 80% TiO$_2$, and (c) 3–44% ZnO + 56% TiO$_2$. The control consisted of a mixture of varnish and water, used to assess the occurrence of direct photolysis by solar radiation.

Oxide mixtures were homogenized for 60 min using a basic analytical mill (IKA A11) and then suspended in water. In parallel, CMC and PAA–NH$_4$ were solubilized in deionized water. Subsequently, the solution was mixed with paint by using a mechanical agitator simultaneously with an ultrasound. Mixtures were stirred for 15 min for homogenization.

Figure 1a–c shows the structure assembled for painting the plates. In this step, a spray gun (DeVilbiss JGA-503), a dual air filter regulator (DeVilbiss FRC-600), and an air compressor (SCHULZ Classic, mobile MSL) were used.
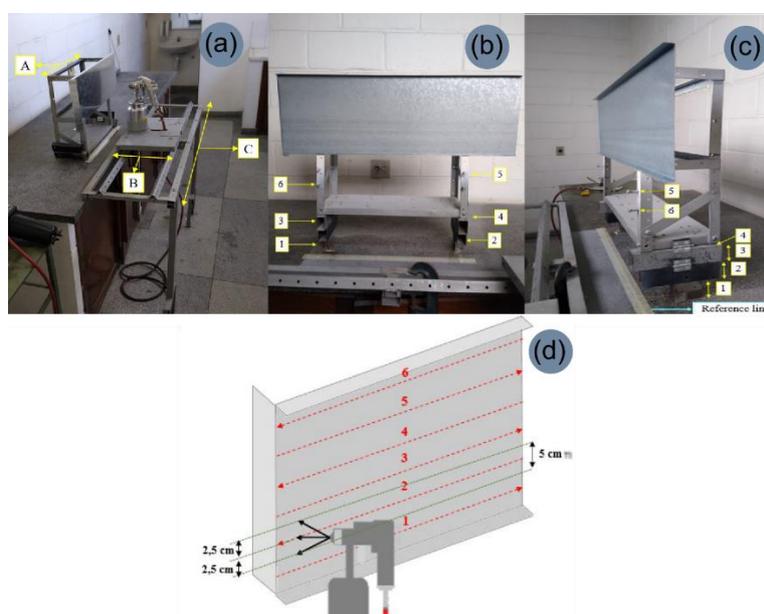
Figure 1. Paint lab assembled for the present study: **a)** Painting system consisting of a (A) sample holder, (B) mobile car with spray gun, and (C) fixed structure; **b)** Front view of the sample holder with a $750 \times 250 \times 0.5$ mm galvanized steel plate and six height adjustments; **c)** Side view of the sample holder with the six height adjustments and a reference line; **d)** Schematic (not to scale) showing the horizontal motion of the spray gun along the galvanized steel plate at heights 1 to 6 to complete a coating.
Source: Nohara *et al.* (2022).

Figure 1b and c shows the six height adjustment points of the sample holder, equally spaced at 5 cm. The adjustments are placed in such a manner so as to allow for overlay painting. Position number 1 consists of a solid metal bracket measuring 2.5 cm in height, resulting in a total distance of 25 cm between the upper end of the metal plate and the reference line (marked in blue in Figure 1c). By removal of the solid metal support at position 1, position 2 is achieved. Position 3 is achieved by removing the support at position 2, and position 4 is achieved by removing the support at position 3. Position 5 is achieved by positioning the lower end of the plate at height 5, and position 6 is achieved by positioning the lower end of the plate at height 6.

The distance between the reference line and the gun nozzle was 20 cm. Suspensions were applied by horizontal spraying on four different galvanized steel plates measuring $750 \times 250 \times 0.5$ mm each (Figure 1b). The vertical fan of the spray gun was adjusted to 5.0 cm height. The following instructions exemplify the application of the first stroke of the first coating: (i) adjust the galvanized steel plate to height position 1, (ii) securely attach the paint sprayer to the sliding track (placed at 90° to the plate), (iii) bring the sliding track to the left side (beginning) of the fixed structure, and (iv) move the sliding track to the right side, covering a distance of 750 mm in 4.0 s at constant speed with the trigger pulled to the desired pressure. After this procedure, the galvanized steel plate is set to height position 2, and the second stroke is applied in the opposite direction (from right to left). Each coating consisted of six strokes.

Figure 1d shows the six preset positions of the spray gun along the galvanized steel plate and the direction of each stroke. The figure also highlights the area covered by stroke 2. Note that each stroke overlaps 50% of the area covered by the previous stroke. Nine coatings of suspension were applied per sample. The first coating was semi-wet and applied at 40 psi. This procedure ensured the deposition of a uniform coating without coalescence of droplets. The remaining eight coatings were wet and applied at 20 psi, forming a continuous, uniform film of coalescent droplets. At the end of the procedure, film thickness was measured using a Mitutoyo digital micrometer. Films had a mean thickness of 600 ± 80 µm.

Leachate was collected from the municipal landfill of Cachoeira Paulista, São Paulo State, Brazil (22°39′4″ S 45°3′18″ W). After collection, the sample (100 L) was homogenized by mechanical stirring and stored in a cold room at 4°C until use. The physicochemical characteristics of leachate samples, namely chemical oxygen demand (COD), biochemical oxygen demand (BOD), total organic carbon (TOC), fixed and volatile solids, organic and ammoniacal nitrogen, phenols, residual peroxide, oils and greases, color, pH, and turbidity (Table A1), were determined according to standard methods (APHA *et al.*, 2017).

Photocatalytic tests were performed on bench-scale thin-film fixed-bed reactors operated in continuous recirculation mode under solar irradiation. Reactors were positioned in the direction of the Equator at an inclination angle of 23° (Figure 2).
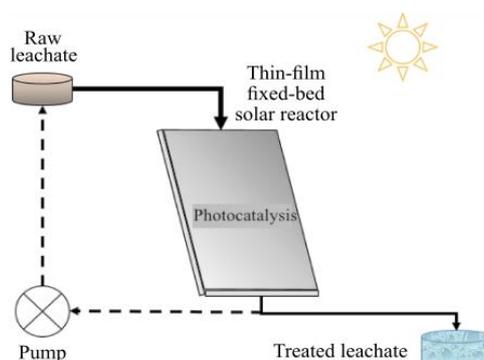
Figure 2. Thin-film fixed-bed solar reactor used in heterogeneous photocatalytic experiments.

The total volume of fresh leachate used during the experiments was 3 L. The flow rate was maintained at 12–13 L min^{-1}. Reactions were run between 11:00 h and 15:00 h during 5 days with sunny weather and temperatures ranging from 28 to 32°C in autumn. Solar irradiance was measured by using an ILT 1400A International Light radiometer, which recorded values of 750–872 mJ cm^{-2} at the end of each operation. The mean evaporation rate of leachate during an experimental cycle was 160 mL; this volume was replaced with water, added in 20 mL aliquots every 30 min during the photocatalytic process. Before the beginning of the experiment, the pH of fresh leachate was measured (pH = 7.8–8.0) and adjusted according to the experimental design by adding small portions of 98% (w/w) sulfuric acid (H$_2$SO$_4$). pH adjustments during photocatalysis were performed with 10 mol L^{-1} H$_2$SO$_4$ solution, added directly to the reactor reservoir. Aliquots from the reservoir were collected every 20 min for pH control and adjustment during operation. During the photocatalytic process, treated leachate was collected every 5 min for the first 20 min and then every 10 min until 240 min of reaction, totaling 26 samples per experiment.

To assess possible effects of non-catalyzed photolysis on degradation, we performed a control test without addition of oxides or additives. A sample aliquot was collected at the beginning and another at the end of the reaction (240 min). Environmental conditions (temperature, leachate volume, and solar irradiation) were similar to those of other experiments. The control test indicated minimal occurrence of photolytic degradation.

Separation of humic substances was performed according to the method described by APHA *et al.* (2017). Separation steps are illustrated in Figure A1. Analytical characterization of humic substances was carried out on a Shimadzu TOC-V system by the total combustion method (680°C) with non-dispersive infrared detection. The equipment can determine total carbon, inorganic carbon, TOC, and non-purgeable organic carbon in aqueous samples within the concentration range of 2.0 to 1,000 mg L^{-1}. TOC is obtained by subtraction of inorganic carbon from total carbon. Inorganic carbon is determined by acidification of samples and consequent conversion of carbonates into CO$_2$, which was shown to be negligible in preliminary analyses. Finally, the remaining fraction is quantified as non-purgeable organic carbon. It should be noted that HA was determined separately from FAH.

A 2^2 full factorial experimental design was used, with one replication of each run and two replications of the center point, totaling 10 runs grouped under conditions I to V (Table 1). Three ZnO–TiO$_2$ mixtures (80% TiO$_2$, 56% TiO$_2$, and 35% TiO$_2$) and three pH ranges (4.5–5.0, 6.0–6.5, and 7.5–8.0) were evaluated. Materials containing only TiO$_2$ or ZnO were not assessed, as previous studies indicated that these compounds have similar degradation efficiencies for the evaluated organic fractions. It is necessary, however, to explore different proportions of semiconductors for optimization.

Table 1. Experiments, factors, and levels.

Conditions	Runs	Factor	
		[pH]	[ZnO–TiO$_2$]
I	1 and 5	4.5–5.0 (−1)	80% TiO$_2$ (−1)
II	2 and 6	4.5–5.0 (−1)	35% TiO$_2$ (+1)
III	3 and 7	7.5–8.0 (+1)	80% TiO$_2$ (−1)
IV	4 and 8	7.5–8.0 (+1)	35% TiO$_2$ (+1)
V	9 and 10	6.0–6.5 (0)	56% TiO$_2$ (0)

[pH], pH value; [ZnO–TiO$_2$], concentration of the binary mixture. Numbers in parentheses indicate coded levels for pH values or concentration.

As already mentioned, the treated leachate was collected until 240 min of reaction. Sample

Rev. Ambient. Água vol. 18, e2932 - Taubaté 2023

IPABH

withdrawal did not affect reaction kinetics. A reaction volume of 0.47 L and a volumetric flow rate of 12.5 L min^{-1} were considered for simulations. A simplified first-order kinetics was used to compare the intrinsic reaction rate between systems. Equations 7 and 8 describe the plug flow reactor and stirred tank stages, respectively.

$$C_i = C_{i_0} exp\left(-k_i \frac{V}{v_0}\right) \tag{7}$$

$$\frac{dC_i}{dt} = \frac{v_0}{V}\left(C_i - C_{i_0}\right) \tag{8}$$

Where C_{io} = concentration of i at the plug flow reactor inlet, C_i = concentration of i at the plug flow reactor outlet, k_i= oxidation rate constant of i, V = plug flow reactor volume, v_0= volumetric flow rate, t = time and i = HA or FAH.

Model fits were obtained by using the ode algorithm in Scilab version 6.1.1.

3. RESULTS AND DISCUSSION

The procedure adopted here for coating (overlapping) allowed obtaining films with high thickness (600 ± 80 µm). Such thickness is in line with the recommendations of Samanamud *et al.* (2012). High thickness is an important characteristic, as it is associated with coat durability and reduced operation and production costs. However, no study has yet assessed the durability of similar films. The paints formulated for the thin-film fixed-bed reactor (galvanized steel test bodies) were prepared by our group using an innovative method. It is worth emphasizing that the paints had low additive concentration and good load distribution.

Table 2 shows the results of HA and FAH removal efficiencies. The highest HA removal efficiency (62% ± 4.9%) was achieved under experimental Condition I, that is, in acidic medium with a high TiO$_2$ concentration. The highest FAH removal efficiency (16% ± 4.2%) was obtained under experimental Condition II, characterized by high ZnO concentration and acidic medium. Such results demonstrate that it is important to use mixtures of these two catalysts to degrade different groups of recalcitrant humic substances.

Table 2. Removal efficiency of humic acids (HA) and fulvic acids + humins (FAH).

Experimental condition	[pH]	[ZnO–TiO2]	Substance	Removal efficiency (%), mean ± SD
I	(−1)	(−1)	HA	62 ± 4.9
			FAH	13 ± 4.2
II	(+1)	(+1)	HA	44 ± 4.9
			FAH	16 ± 4.2
III	(−1)	(−1)	HA	41 ± 4.9
			FAH	29 ± 4.2
IV	(+1)	(+1)	HA	52 ± 2.8
			FAH	24 ± 2.8
V	(0)	(0)	HA	39 ± 2.1
			FAH	16 ± 4.2

Levels for [pH]: (−1) = 4.5–5.0, (0) = 6.0–6.5, and (+1) = 7.5–8.0. Levels for [ZnO–TiO2]: (−1) = 80% TiO2, (0) = 50% TiO2, and (+1) = 35% TiO2.
Source: adapted from Nohara *et al.* (2022).

IPABH

Curve fits for the tested experimental conditions (Equations 1 and 2)) are depicted in Figure 3. Mean R^2 values were calculated for curve fits, with $R^2 = 0.984$ for HA and $R^2 = 0.964$ for FAH.
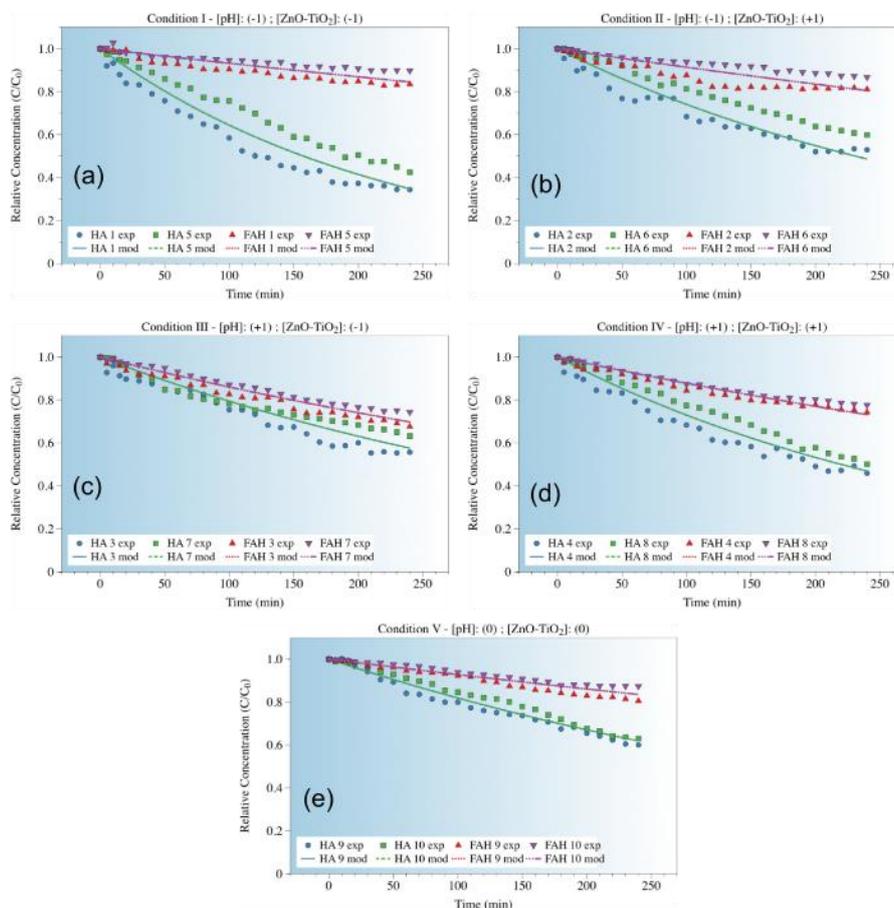
Figure 3. Curve fits for experimental Conditions I to V (a–e). HA, humic acids; FAH, fulvic acids + humins; exp, experimental data; mod, model fit. For [pH]: (−1) = 4.5–5.0, (0) = 6.0–6.5, and (+1) = 7.5–8.0. For [ZnO/TiO2]: (−1) = 80% TiO2, (0) = 56% TiO2, and (+1) = 35% TiO2 (see Table 1).

The rate constants fitted in this study are listed in Table 3. It can be seen that kinetic parameters did not vary greatly as a function of pH range or catalyst system. Therefore, we applied analysis of variance (ANOVA) to assess the significance of these variables in organic fraction degradation. However, differences as a function of contaminant type (HA or FAH) are evident.

Table 3. First-order rate constants.

Constant	Experimental Conditions (runs)				
	I (1 and 5)	II (2 and 6)	III (3 and 7)	IV (4 and 8)	V (9 and 10)
k_{HA} (min^{-1})	4.4×10^{-3}	3.0×10^{-3}	2.3×10^{-3}	3.1×10^{-3}	2.0×10^{-3}
k_{FAH} (min^{-1})	7.0×10^{-4}	9.0×10^{-4}	1.5×10^{-3}	1.3×10^{-3}	7.5×10^{-4}

k_{HA}, kinetic constant for humic acids; k_{FAH}, kinetic constant for fulvic acids + humins.

A study on HA photodegradation by FeNi$_3$–SiO–TiO$_2$ found a k_{HA} of 15.5×10^{-3} to 220×10^{-3} min^{-1} for HA concentrations in the range of 15 to 2 mg L^{-1}, respectively (Khodadadi *et*

al., 2020). These results indicate that higher HA concentrations lead to lower first-order rate constants. In the current study, we obtained even lower k_{HA} values, which is consistent with the HA concentrations used here (about 600 mg L^{-1}). Oskoei *et al.* (2016) observed similar behavior for UV/ZnO nanophotocatalysis under pH 4: k_{HA} ranged from 0.038 to 0.112 min^{-1} for HA concentrations of 10 to 5 mg L^{-1}, respectively. He (2013) estimated a k_{HA} value of 9.6 $\times$ 10^{-3} min^{-1} for photocatalytic degradation of HA by TiO$_2$ under natural sunlight. The referred process is similar to that applied in the current study, and the findings corroborate those described in Table 1. For solar photocatalysis of HA (68 mg L^{-1}) catalyzed by TiO$_2$ in pH 7.8, a slightly higher k_{HA} value (0.092 min^{-1}) was estimated (Al-Rasheed and Cardin, 2003).

Rajca and Bodzek (2013) studied FA and HA photodegradation by TiO$_2$ and found a k_{HA} value of 0.0025 min^{-1} and a k_{FA} value of 0.0024 min^{-1} for initial HA and FA concentrations of 9.6 and 8.8 mg L^{-1}, respectively. It can be observed that FA rate constants are slightly lower than those for HA. The kinetic data obtained in the current study are in agreement with literature data.

From the ANOVA results presented in Table A2, it was possible to develop a regression model for HA conversion (X_{HA}) after 240 min (Equations 9 and 10) for replicates 1 and 2, respectively). The model had an R^2 of 0.96, with normal distribution of residuals ($p > 0.15$, Kolmogorov–Smirnov test).

$$X_{HA_1} = 0.4130 - 0.03125[ZnO - TiO_2] + 0.1088[ZnO - TiO_2] \times [ZnO - iO_2] + 0.07375[ZnO - TiO_2] \times [pH] \tag{9}$$

$$X_{HA_2} = 0.3570 - 0.03125[ZnO - TiO_2] + 0.1088[ZnO - TiO_2] \times [ZnO - TiO_2] + 0.07375[ZnO - TiO_2] \times [pH] \tag{10}$$

In the model, run replication was considered a categorical variable, given that higher conversions were obtained in the first run (Replicate 1) of each condition than in the second run. The model (Equations 9 and 10) showed that the replicate variable was significant. According to the model, the mean difference in XHA between Replicates 1 and 2 was 5.6% ($0.413 - 0.357 = 0.056$). Such a difference might be due to HA adsorption on the plate painted with the catalyst mixture. We point out that plates were washed with detergent at the end of each run. Thus, it is possible that there was a moderate decrease in HA adsorption after the first run. Liu *et al.* (2008) found that HA has affinity for adsorption onto TiO$_2$ surface, particularly under acidic pH conditions (close to 4.0), because of its point of zero charge and zeta potential. Tran *et al.* (2006) found that carboxylic acids have greater tendency for adsorption, whereas alcohols and long-chain saturated aliphatic compounds do not. Ren *et al.* (2018) explained that adsorption is undesirable and represents an inhibitory factor in photocatalysis. To decrease the occurrence of adsorption onto TiO$_2$, it is necessary to operate under more alkaline pH conditions. However, in this study, we used a pH greater than 4.

ZnO has a positive zeta potential at pH 6.7 to 9.3 (Mohd Omar *et al.*, 2014). HA molecules, in turn, are negatively charged at pH 2.0 to 10.7. With the increase in solution pH (>7.0), HA molecules become more easily ionized because of the action of electrostatic attraction forces (Nguyen *et al.*, 2020). Interestingly, this adsorption potential was observed when the pH was lower than the point of zero charge, resulting from a complex interaction between attractive and repulsive electrostatic forces, van der Waals bonds, and other interactions with humic substances (Mohd Omar *et al.*, 2014). A similar effect was observed in dairy wastewater, as described by Samanamud *et al.* (2012). The authors found enhanced ZnO photocatalytic activity at acidic pH; however, possible adsorption of contaminants onto the semiconductor surface was not discussed.

Another interesting result of ANOVA (Table A2) is the significant interaction between pH and catalyst concentration ($p < 0.001$). The highest XHA value was estimated to be achieved

using acidic pH (−1) and high TiO2 concentration (−1). This result suggests that, for binary mixtures, synergy between compounds favors degradation kinetics. According to the model, the action of TiO2 is favored by acidic medium and that of ZnO by alkaline medium, greatly enhancing absorption of the solar spectrum.

The ANOVA table for FAH conversion (Table A3) allowed the construction of a regression model for FAH conversion (X_{FAH}) after 240 min (Equations 11 and 12) for Replicates 1 and 2, respectively). The model had an R^2 of 0.992, with normal distribution of residuals ($p > 0.15$, Kolmogorov–Smirnov test).

$$X_{FAH_1} = 0.18800 + 0.0600[ZnO - TiO_2] + 0.04500[ZnO - TiO_2] \times [ZnO - TiO_2] - 0.02000[ZnO - TiO_2] \times [pH] \tag{11}$$

$$X_{FA_2} = 0.13200 + 0.0600[ZnO - TiO_2] + 0.04500[ZnO - TiO_2] \times [ZnO - TiO_2] - 0.02000[ZnO - TiO_2] \times [pH] \tag{12}$$

Similar to that found for XHA, the categorical replicate variable was significant in the study of XFAH degradation (Equations 11 and 12) (p < 0.001). The mean difference between XFAH replicate runs was 5.6% (0.188 − 0.132 = 0.056), suggesting that both fractions (FAH and HA) diffused in a similar manner inside catalyst pores. The model suggests an antagonistic behavior in the preference of the catalyst for FAH over HA. This is because, according to the model (Equations 11 and 12)), XFAH is highest at acidic pH (−1) and high ZnO concentration (+1). The finding is corroborated by the kinetic model for humic substance degradation: a higher rate constant for FAH (kFAH = 1.5 × 10−3 min−1) was obtained when using higher ZnO concentrations and acidic pH (4.5–5.0) (condition III), in agreement with the observations of Mohd Omar *et al.* (2014). Thus, the results show a greater affinity of the binary mixture for photocatalytic FAH degradation when high ZnO concentrations are used.

Previous studies have assessed the removal of HA in wastewater using the most diverse treatment techniques. Bekbölet and Balcioglu (1996) investigated the photocatalytic degradation of HA. The authors found that treatment with 1.0 g L^{-1} TiO$_2$ (P25) for 1 h under irradiation removed 40% of TOC and 75% of color (400 nm). In another study, Bekbölet *et al.* (1998) removed color caused by HA in the presence of common inorganic anions (chloride, nitrate, sulfate, and phosphate ions) at pH 6.8. HA was used as an additional matrix for the degradation of some organic contaminants, leading to more than 80% removal of commercial HA by irradiation in the presence of TiO$_2$ (P25) (Minero *et al.*, 1999). Eggins *et al.* (1997) found that TiO$_2$ (P25) under irradiation from a mercury lamp was efficient in reducing HA, achieving about 50% reduction in 12 min.

It is not possible to directly compare our results with those of previous studies, as no study has yet used this mixture of photocatalysts under solar irradiation for the photodegradation of humic substances (separately) in mature leachates. A somewhat similar study was that of Turkten and Bekbölet (2020), who investigated the photodegradation of humic acids (synthesized in the laboratory) by ZnO–TiO$_2$; however, the data were obtained qualitatively, using UV-Vis spectroscopy and fluorescence methods. Other studies on the photodegradation of mature leachate from sanitary landfills obtained similar results; however, they used a greater amount of energy during the process (for material synthesis, intermittent artificial irradiation, etc.) and required additional filtration steps (Jia *et al.*, 2011; Wang *et al.*, 2021). Jia *et al.* (2011). For instance, obtained 60%–97% degradation of dissolved organic carbon using UV + TiO$_2$. Wang *et al.* (2021) applied TiO$_2$ nanoparticles obtained by the solvothermal method for the photodegradation of dissolved organic carbon from mature landfill leachate and achieved a minimum COD reduction of 70%.

The focus of the current study was to decompose recalcitrant substances such as HA and

FA. In general, the resulting compounds, which have low molecular weights, can be readily utilized in bioprocesses. In view of this, only the degradation kinetics of HA and FA were assessed here.

4. CONCLUSION

The paint mixtures formulated in this study were obtained using a successful method. Paints were applied by overlapping coat layers on experimental plates, resulting in films with high thickness. High film thickness is an important characteristic, as it is related to coat durability and reduced operation and production costs.

The highest HA removal efficiency (62% $\pm$ 4.9%) was achieved in acidic medium containing high TiO_2 concentrations, whereas the highest FAH removal efficiency (16% $\pm$ 4.2%) was obtained under high ZnO concentration and acidic conditions.

It should be noted that little is known about the kinetic complexity of leachate treatment by oxidative methods, representing a barrier to process scale-up from benchtop experiments. To better understand the degradation process, we used a first-order kinetic approach. Predictions provided mean R^2 values of 0.984 and 0.964 for HA and FAH degradations, respectively. A rate constant of 2.96×10^{-3} min^{-1} and 1.03×10^{-3} min^{-1} was estimated for HA and FAH degradation, respectively, by considering the best operating conditions for each fraction. The modeling results of the current study are in agreement with literature data and confirm the inverse relationship between contaminant concentration (HA and FAH) and first-order kinetic constants (k_{HA} and k_{FAH}).

The statistical models for HA and FAH degradation had R^2 values of 0.96 and 0.99, respectively. It was possible to observe a significant interaction effect of pH and catalyst concentration on HA and FAH degradation. Statistical and kinetic models suggest that HA degradation is higher under acidic pH and high TiO_2 concentration conditions. For FAH, degradation is favored at acidic pH and high ZnO concentrations. The model also revealed a significant difference of 5.6% between replicates, attributed to initial adsorption of wastewater onto the photocatalytic reactor plate in the first run.

In addition to the experimental evidence, both kinetic and statistical models proved the importance of mixing the two catalysts for effective degradation of humic substances. The results confirm that the proposed method for developing photocatalytic materials was successful and shows promise because of its ease of preparation and low input requirements. Future studies should assess the biodegradability of leachate as a complementary step to the treatment process.

5. ABBREVIATIONS

ANOVA – Analysis of variance

AOPs – Advanced oxidation processes

C_{i_0} – Concentration of species i at the plug flow reactor inlet

C_i – Concentration of species i at the plug flow reactor outlet

CMC – Carboxymethylcellulose

CO_2 – Carbon dioxide

FAH – Fulvic acid + humins

HA – Humic acid

H_2SO_4 – Sulfuric acid

i – Subscript indicating HA or FAH

k_{FAH} – Kinetic constant for fulvic acids + humins

k_{HA} – Kinetic constant for humic acids

k_i – Oxidation rate constant of species i

PAA–NH$_4$ – Ammonium polyacrylate

pH – Hydrogen potential

[pH] – pH value

R^2 – Coefficient of determination

SD – Standard deviation

t – Time

TiO$_2$ – Titanium dioxide

V – Plug flow reactor volume

v_0 – Volumetric flow rate

X_{FAH} – FAH conversion

X_{HA} – HA conversion

ZnO – Zinc oxide

ZnO–TiO$_2$ – Binary mixture of ZnO and TiO$_2$

[ZnO–TiO$_2$] – Concentration of the binary mixture

6. REFERENCES

AL-RASHEED, R.; CARDIN, D. J. Photocatalytic degradation of humic acid in saline waters. Part 1. Artificial seawater: influence of TiO$_2$, temperature, pH, and air-flow. **Chemosphere**, v. 51, n. 9, p. 925–933, 2003. https://doi.org/10.1016/S0045-6535(03)00097-3

APHA; AWWA; WEF. **Standard Methods for the examination of water and wastewater**. 23nd ed. Washington, 2017. 1504 p.

BAH, A.; CHEN, Z.; BAH, A.; QIAN, Q.; TUAN, P. D.; FENG, D. Systematic literature review of solar-powered landfill leachate sanitation: Challenges and research directions over the past decade. **Journal of Environmental Management**, v. 326, part B., e116251, 2023. https://doi.org/10.1016/j.jenvman.2022.116751.

BEKBÖLET, M.; BALCIOGLU, I. Photocatalytic degradation kinetics of humic acid in aqueous TiO dispersions: The influence of hydrogen peroxide and bicarbonate ion. **Water Science and Technology**, v. 34, n. 9, 1996. https://doi.org/10.1016/S0273-1223(96)00789-5.

BEKBÖLET, M.; BOYACIOGLU, Z.; ÖZKARAOVA, B. The influence of solution matrix on the photocatalytic removal of color from natural waters. Water Science and Technology, v. 38, n. 6, 1998. https://doi.org/10.1016/S0273-1223(98)00577-0.

BRITO, R. A.; ISÁRIO FILHO, H. J.; AGUIAR, L. G.; ALCÂNTARA, M. A. K.; SIQUEIRA, A. F.; RÓS, P. C. M. D. Degradation Kinetics of Landfill Leachate by Continuous-Flow Catalytic Ozonation. **Industrial & Engineering Chemistry Research**, v. 58, n. 23, p. 9855–9863, 2019. https://doi.org/10.1021/acs.iecr.9b01391.

Rev. Ambient. Água vol. 18, e2932 - Taubaté 2023

IPABH

BYRNE, C.; SUBRAMANIAN, G.; PILLAI, S. C. Recent advances in photocatalysis for environmental applications. **Journal of Environmental Chemical Engineering**, v. 6, n. 3, p. 3531–3555, 2018. https://doi.org/10.1016/j.jece.2017.07.080.

COSTA, A. M.; ALFAIA, R. G. DE S. M.; CAMPOS, J. C. Landfill leachate treatment in Brazil – An overview. **Journal of Environmental Management**, v. 232, p. 110–116, 2019. https://doi.org/10.1016/j.jenvman.2018.11.006.

DI MAURO, A.; FRAGALÀ, M. E.; PRIVITERA, V.; IMPELLIZZERI, G. ZnO for application in photocatalysis: From thin films to nanostructures. **Materials Science in Semiconductor Processing**, v. 69, p. 44–51, 2017. https://doi.org/10.1016/j.mssp.2017.03.029.

EGGINS, B.; FIONA, L. P.; BYRNE, J. A. Photocatalytic treatment of humic substances in drinking water. **Water Research**, v. 31, n. 5, p. 1223–1226, 1997. https://doi.org/10.1016/S0043-1354(96)00341-7.

HASSAN, M.; ZHAO, Y.; XIE, B. Employing TiO_2 photocatalysis to deal with landfill leachate: Current status and development. **Chemical Engineering Journal**, v. 285, p. 264–275, 2016. https://doi.org/10.1016/j.cej.2015.09.093.

HE, Y. Titanium Dioxide-Mediated Photocatalytic Degradation of Humic Acid under Natural Sunlight. **Water Environment Research**, v. 85, n. 1, p. 3–12, 2013. https://doi.org/10.2175/106143012x13378023685790.

JIA, C.; WANG, Y.; ZHANG, C.; QIN, Q. UV-TiO2 Photocatalytic Degradation of Landfill Leachate. **Water, Air & Soil Pollution**, v. 217, p. 375-385, 2011. https://doi.org/10.1007/s11270-010-0594-7.

JONES, F. N.; NICHOLS, M. E.; PAPPAS, S. P. **Organic coatings: science and technology**. 4rd ed. Hoboken: John Wiley & Sons, 2017.

KHODADADI, M.; AL-MUSAWI, T. J.; KAMANI, H.; SILVA, M. F.; PANAHI, A. H. The practical utility of the synthesis FeNi3@SiO2@TiO2 magnetic nanoparticles as an efficient photocatalyst for the humic acid degradation. **Chemosphere**, v. 239, p. 124723, 2020. https://doi.org/10.1016/j.chemosphere.2019.124723.

LI, B.; YUAN, D.; GAO, C.; ZHANG, H.; LI, Z. Synthesis and characterization of TiO_2/ZnO heterostructural composite for ultraviolet photocatalytic degrading DOM in landfill leachate. **Environmental Science and Pollution Research**, v. 29, p. 85510–85524, 2022. https://doi.org/10.1007/s11356-022-21758-x.

LIU, S.; LIM, M.; FABRIS, R.; CHOW, C.; CHIANG, K.; DRIKAS, M.; AMAL, R. Removal of humic acid using TiO2 photocatalytic process – Fractionation and molecular weight characterisation studies. **Chemosphere**, v. 72, n. 2, p. 263–271, 2008. https://doi.org/10.1016/j.chemosphere.2008.01.061.

LUO, H.; ZENG, Y.; CHENG, Y.; HE, D.; PAN, X. Recent advances in municipal landfill leachate: A review focusing on its characteristics, treatment, and toxicity assessment. **Science of The Total Environment**, v. 703, p. 135468, 2020. https://doi.org/10.1016/j.scitotenv.2019.135468.

IPABH

MINERO, C.; PELIZZETTI, E.; SEGA, M.; FRIBERG, S. E. The role of humic substances in the photocatalytic degradation of water contaminants. **Journal of Dispersion Science and Technology**, v. 20, n. 1–2, p. 643–661, 1999. https://doi.org/10.1080/01932699908943812.

MOHD OMAR, F.; ABDUL AZIZ, H.; STOLL, S. Aggregation and disaggregation of ZnO nanoparticles: Influence of pH and adsorption of Suwannee River humic acid. **Science of The Total Environment**, v. 468–469, p. 195–201, 2014. https://doi.org/10.1016/j.scitotenv.2013.08.044.

NGUYEN, T. T.; NAM, S.-N.; KIM, J.; OH, J. Photocatalytic degradation of dissolved organic matter under ZnO-catalyzed artificial sunlight irradiation system. **Scientific Reports**, v. 10, n. 1, p. 13090, 2020. https://doi.org/10.1038/s41598-020-69115-7.

NOHARA, N. M. L.; IZÁRIO FILHO, H. J.; ALCÂNTARA, M. A. K.; OLIVEIRA, G. C. K. de; VERNILLI JUNIOR, F.; NOHARA, E. L. *et al.* Binary Mixtures of ZnO/TiO2 for Solar Heterogeneous Photocatalysis of Non-Purgeable Organic Carbon in Landfill Leachate. **Research, Society and Development**, v. 11, n. 6, p. e48411624570, 2022. http://dx.doi.org/10.33448/rsd-v11i6.24570.

OSKOEI, V.; DEHGHANI, M. H.; NAZMARA, S.; HEIBATI, B.; ASIF, M.; TYAGI, I. *et al.* Removal of humic acid from aqueous solution using UV/ZnO nano-photocatalysis and adsorption. **Journal of Molecular Liquids**, v. 213, p. 374–380, 2016. https://doi.org/10.1016/j.molliq.2015.07.052.

PENG, Y. Perspectives on technology for landfill leachate treatment. **Arabian Journal of Chemistry**, v. 10, p. S2567–S2574, 2017. https://doi.org/10.1016/j.arabjc.2013.09.031.

RAJCA, M.; BODZEK, M. Kinetics of fulvic and humic acids photodegradation in water solutions. **Separation and Purification Technology**, v. 120, p. 35–42, 2013. https://doi.org/10.1016/j.seppur.2013.09.019.

REN, M.; DROSOS, M.; FRIMMEL, F. H. Inhibitory effect of NOM in photocatalysis process: Explanation and resolution. **Chemical Engineering Journal**, v. 334, p. 968–975, 2018. https://doi.org/10.1016/j.cej.2017.10.099.

SAMANAMUD, G. R. L.; LOURES, C. C. A.; SOUZA, A. L.; SALAZAR, R. F. S.; OLIVEIRA, I. S.; SILVA, M. B. *et al.* Heterogeneous Photocatalytic Degradation of Dairy Wastewater Using Immobilized ZnO. **ISRN Chemical Engineering**, v. 2012, p. 1–8, 2012. https://doi.org/10.5402/2012/275371.

SELCUK, H.; SENE, J. J.; ANDERSON, M. A. Photoelectrocatalytic humic acid degradation kinetics and effect of pH, applied potential and inorganic ions. **Journal of Chemical Technology & Biotechnology**, v. 78, n. 9, p. 979–984, 2003. https://doi.org/10.1002/jctb.895.

SILVA, T. F. C. V. PERI, P.; FAJARDO, A. S.; PAULISTA, L. O.; SOARES, P. A.; MARTÍNEZ-HUITLE, C.A.; VILAR, V. J. P. Solar-driven heterogeneous photocatalysis using a static mixer as TiO2-P25 support: Impact of reflector optics and material. **Chemical Engineering Journal**, v. 435, p. 134831, 2022. https://doi.org/10.1016/j.cej.2022.134831.

Rev. Ambient. Água vol. 18, e2932 - Taubaté 2023

IPABH

SONG, J.; SHI, M.; XIA, L.; DAI, J.; LUO, L.; WANG, H. *et al.* The comparative study on inhibitory effect of natural organic matters on the TiO2 and activated carbon/TiO2 composites for the removal of 17α-ethinylestradiol. **Chemosphere**, v. 333, p. 138930, 2023. https://doi.org/10.1016/j.chemosphere.2023.138930.

TAIT, P. W.; BREW, J.; CHE, A.; COSTANZO, A.; DANYLUK, A.; DAVIS, M. *et al.* The health impacts of waste incineration: a systematic review. **Australian and New Zealand Journal of Public Health**, v. 44, n. 1, p. 40–48, 2020. https://doi.org/10.1111/1753-6405.12939.

TRAN, H.; SCOTT, J.; CHIANG, K.; AMAL, R. Clarifying the role of silver deposits on titania for the photocatalytic mineralisation of organic compounds. **Journal of Photochemistry and Photobiology A: Chemistry**, v. 183, n. 1–2, p. 41–52, 2006. https://doi.org/10.1016/j.jphotochem.2006.02.018.

TURKTEN, N.; BEKBÖLET, M. Photocatalytic performance of titanium dioxide and zinc oxide binary system on degradation of humic matter. **Journal of Photochemistry and Photobiology A: Chemistry**, v. 401, p. 112748, 2020. https://doi.org/10.1016/j.jphotochem.2020.112748.

WANG, C.; SUN, X.; SHAN, H.; ZHANG, H.; XI, B. Degradation of Landfill Leachate Using UV-TiO2 Photocatalysis Combination with Aged Waste Reactors. **Processes**, v. 9, n. 6, p. 946-959, 2021. https://doi.org/10.3390/pr9060946.

WANG, X.; WU, Z.; WANG, Y.; WANG, W.; WANG, X.; BU, Y. *et al.* Adsorption–photodegradation of humic acid in water by using ZnO coupled TiO$_2$/bamboo charcoal under visible light irradiation. **Journal of Hazardous Materials**, v. 262, p. 16-24, 2013. https://doi.org/10.1016/j.jhazmat.2013.08.037.

XUE, G.; LIU, H.; CHEN, Q.; HILLS, C.; TYRER, M.; INNOCENT, F. Synergy between surface adsorption and photocatalysis during degradation of humic acid on TiO2/activated carbon composites. **Journal of Hazardous Materials**, v. 186, n. 1, p. 765–772, 2011. https://doi.org/10.1016/j.jhazmat.2010.11.063.

YE, J.; HU, A.; REN, G.; CHEN, M.; TANG, J.; ZHANG, P. *et al.* Enhancing sludge methanogenesis with improved redox activity of extracellular polymeric substances by hematite in red mud. **Water Research**, v. 134, p. 54–62, 2018. https://doi.org/10.1016/j.watres.2018.01.062.

ZULFIKAR, M. A.; CHANDRA, A. D.; RUSNADI; SETIYANTO, H.; HANDAYANI, N.; WAHYUNINGRUM, D. TiO$_2$/ZnO nanocomposite photocatalyst: Synthesis, characterization and their application for degradation of humic acid from aqueous solution. **Songklanakarin Journal of Science and Technology**, v. 42, n. 2, p. 439-446, 2020. https://doi.org/10.14456/sjst-psu.2020.57.

7. APPENDICES

Figure A1 illustrates the separation of humic substances performed according to the method described by APHA (2017).

IPABH
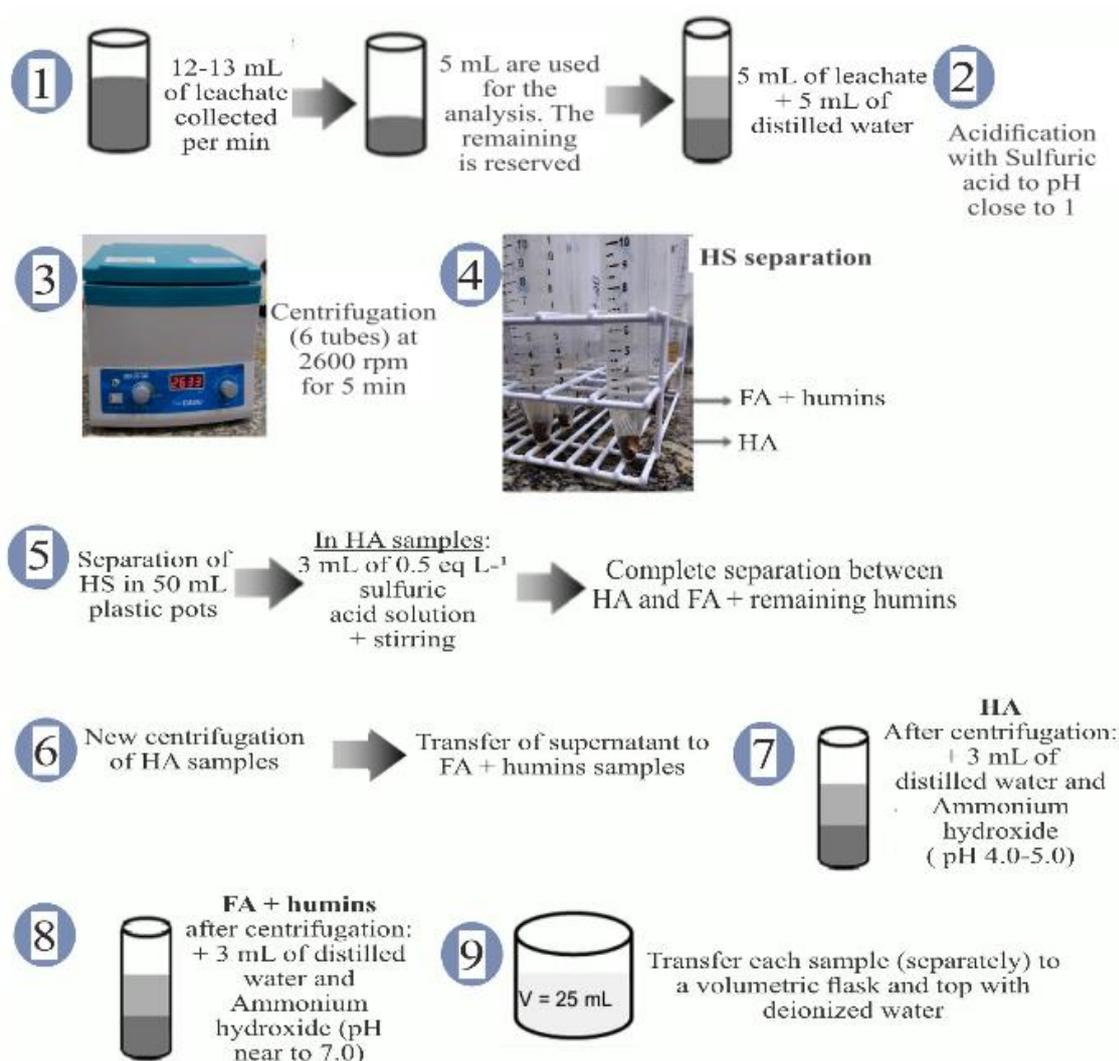
Figure A1. Separation of humic substances (HS). FA, fulvic acids; HA, humic acids.
Source: adapted from APHA (2017).

Table A1 presents the physicochemical characteristics of mature leachate and the regulatory requirements for disposal, as determined in CETESB (2007) Resolution Article 18 and CONAMA (2005). The results found for the amount of COD, 4541.24 mg L^{-1}, is considered high, but the factors related to the types of residues, climate and the form of final disposal of residues must be taken into consideration. The pH of the leachate undergoes large variations depending on the residues degradation phase. Alkalinity may occur due to the presence of bicarbonates, carbonates or hydroxides and represents the ability of the medium to resist possible variations of pH. Regarding oils and greases, there is a limit established by federal law: mineral oils up to 20 mg L^{-1} and animal and vegetable oils up to 50 mg L^{-1}. The value found for the analyzed leachate is above the maximum allowed limit. For parameters without limitation of maximum concentration, there is a marked change in the ammoniacal nitrogen parameters, phenol, oils and greases and turbidity.

Table A1. Analytical parameters of landfill leachate and regulatory requirements for disposal according to Brazilian legislation.

Parameter	Value	CETESB 2007 Resolution, Article 18	CONAMA Resolutions Nos. 357/05 and 430/11
COD ($mg\ L^{-1}$)	4541.24	-	-
BOD$_5$ ($mg\ L^{-1}$)	-	Up to 60 mg/L or above 80% removal	Above 60% removal
TOC ($mg\ L^{-1}$)	1471.11	-	
Ammoniacal nitrogen ($mg\ L^{-1}$)	1262.49	-	20
Organic nitrogen ($mg\ L^{-1}$)	11.49	-	-
Phenol ($mg\ L^{-1}$)	164.34	-	-
Residual peroxide	0	-	-
Oils and greases ($mg\ L^{-1}$)	726	20	50
Color (Pt-Co units $mg^{-1}\ L^{-1}$)	5711.41	-	75
pH	9	5.0–9.0	5.0–9.0
Turbidity (NTU)	302	40	100

(-) There is no regulatory requirement for the parameter.

Tables A2 and A3 present the analysis of variance for the photocatalytic degradation of HA and FAH, respectively.

Table A2. Analysis of variance for humic acid degradation.

Source	df	Adj SS	Adj MS	*F*-value	*P*-value
Regression	4	0.078088	0.019522	33.98	0.001
[ZnO–TiO$_2$]	1	0.007812	0.007812	13.60	0.014
Replicate	1	0.007840	0.007840	13.65	0.014
[ZnO–TiO$_2$] × [ZnO–TiO$_2$]	1	0.018922	0.018922	32.94	0.002
[ZnO–TiO$_2$] × [pH]	1	0.043513	0.043513	75.74	0.000
Error	5	0.002873	0.000575		
Total	9	0.080960			

$S = 0.0239687$. $R^2 = 96.45\%$. Adjusted $R^2 = 93.61\%$.
Predicted $R^2 = 86.03\%$.

IPABH

Table A3. Analysis of variance for fulvic acid + humin degradation.

Source	df	Adj SS	Adj MS	*F*-value	*P*-value
Regression	4	0.043080	0.010770	149.58	0.000
[ZnO–TiO$_2$]	1	0.028800	0.028800	400.00	0.000
Replicate	1	0.007840	0.007840	108.89	0.000
[ZnO–TiO$_2$] × [ZnO–TiO$_2$]	1	0.003240	0.003240	45.00	0.001
[ZnO–TiO$_2$] × [pH]	1	0.003200	0.003200	44.44	0.001
Error	5	0.000360	0.000072		
Total	9	0.043440			

$S = 0.0084853$. $R^2 = 99.17\%$. Adjusted $R^2 = 98.51\%$. Predicted $R^2 = 96.94\%$.